Modeling and Control of Convertible Micro Air Vehicles

P. Morin*
Institut des Systèmes Intelligents et de Robotique (ISIR)
Sorbonne Universités, UPMC Univ. Paris 06, CNRS UMR 7222
4 Place Jussieu, 75252 Paris Cedex, France
E-mail address: *morin@isir.upmc.fr*

Abstract

Convertible UAVs (Unmanned Aerial Vehicles) associate the capacities of stationary flight, like helicopters, and efficient cruising flight, like airplanes. This duality is usually achieved by a mechanical design that combines several propellers and wings. A large variety of such combinations have been proposed, especially after the Second World War. Thanks to electronic miniaturization, recent years have seen a revival of the research on this topic through convertible MAVs (Micro Air Vehicles). This paper provides an overview of existing structures and associated modeling and feedback control issues.

1 Introduction

So many types of aerial vehicles have been developed that their classification is doomed to failure. Nevertheless, fixed-wing aircraft (e.g., airplanes), rotary-wing aircraft (e.g., helicopters), flapping-wing aircraft (e.g., bird-like), and lighter-than-air aircraft (e.g., blimps), certainly form the main classes to be encountered. This classification is not strict and many combinations can be imagined. This paper is dedicated to convertible aircraft, that belong to both the fixed-wing and rotary-wing categories. In other words, these vehicles can perform Vertical Take-Off and Landing (VTOL) thanks to one or several propellers and they are also endowed with fixed-wing(s) so as to benefit from lift at high speed.

First prototypes of convertible aircraft were built after the Second World War, like the Vertol VZ-2 Tilt-Wing of the US Navy (Fig. 1 below), the XFY Pogo Tail-Sitter of the US Navy (Fig. 2 below), or the Coleoptere Tail-Sitter of the French company SNECMA (Fig. 3 below). These early developments had to face several difficulties, among which the transition from hover to cruising flight. Tail-sitters were particularly challenging for the pilot: the take-off position was very uncomfortable with no downward visibility. These systems gave rise to many accidents, which prematurely ended several research programs, like SNECMA's Coleoptere. Tilt-wing configurations were closer to the standard airplane and helicopter configurations and therefore easier to fly. Another alternative was to use standard airplane configuration with vectorized thrust. Many military combat aircraft of this type were built around the sixties like the British Hawker Siddeley Harrier (Fig. 4), which was the first commercialized combat aircraft with VTOL capacities. These vehicles do not exactly satisfy the above definition of a convertible aircraft since they are propelled by jets instead of propellers but they share the same operational characteristics. Another direction was to design convertible aircraft from helicopter structures. Several attempts in this direction have been made, like the Sikorsky Xwing of the late seventies (Fig. 5) below, or the more recent Eurocopter-X3 (Fig. 6).

Miniaturization and cost reduction of electronic components have dramatically modified the picture in the last twenty years. MAVs (Micro Air Vehicles) can now be built at a very low cost. Some of the concepts developed in the twentieth century for manned aircraft can be tested on scale models, with a tremendous reduction of cost and risk. Many convertible MAV structures are inherited from the post Second World War developments on full scale aircraft but new configurations can also be proposed thanks to the different scale and the absence of a pilot aboard. However, the mechanical complexity of structures like the Harrier, the Sikorsky Xwing, or the Eurocopter-X3 also seem to have prevented the design of equivalent scale-models. In other words, the class of convertible MAVs differs

*This work has been supported by the "Chaire d'excellence en Robotique RTE-UPMC".

from that of full-scale convertible aircraft.

Convertible MAVs present several challenges, from the mechanical design to (semi-)autonomous flight tests. Like any other aerial vehicle, designing a convertible MAV requires a minimal understanding of aerodynamics. Compared to now omnipresent quadrotors, combination of fixed and rotary-wings adds significant complexity with aerodynamic interactions that may endanger both energy performance and stability. Energy efficiency is clearly the main incentive for using a convertible MAV instead of a classical quadrotor. However, this is always a matter of compromise since a convertible MAV (with equivalent rotor diameters) will always be less efficient than a quadrotor in hover, due to the wings' weight, and less efficient than an airplane in cruising flight, due additional propellers. Depending on the mission, different configurations should be preferred. Complex design methodologies have been developed to address these VTOLs' pre-sizing issues[1].

Feedback control is another challenge. From the early developments of convertible aircraft of the fiftieths, control of such vehicles is known to be a critical issue, in particular for tail-sitters. The difficulty is increased for MAVs due to their small size and high sensibility to wind. Flight at large angles of attack is more likely to occur in this case and the standard linear models of lift and drag used for airplanes' wings are no longer valid. Furthermore, unsteady aerodynamic effects associated with MAVs' fast rotational dynamics is another possible source of complexity [3]. To the author's opinion, we are still at the beginning of the investigation of such issues from the control point of view. The main objective of this paper is to provide an introduction to the topic of convertible MAVs from a control/robotics point of view, and suggest research directions.

The paper is organized as follows. Section 2 provides an overview of existing convertible concepts for both full-scale and MAV aircraft. Section 3 discusses modeling aspects and specificities of MAVs. Section 4 is dedicated to the feedback control of these vehicles. Finally, concluding remarks and perspectives are given in the conclusion.

2 Overview of convertible MAV structures

Tilt-bodies and Tilt-rotors/Tilt-wings are the two main classes of convertible MAVs. A larger classification of VTOL vehicles, independently of their size, can be found in [1] but as indicated above, some full-

Figure 1: Vertol VZ-2 Tilt-Wing

Figure 2: XFY Pogo Tail-Sitter

Figure 3: Coleoptere Tail-Sitter

Figure 4: Harrier thrust-vectorized aircraft

Figure 5: Sikorsky Xwing

Figure 6: Eurocopter X3

scale aircraft have not been built at the MAV scale.

Tilt-bodies are essentially airplanes with sufficient thrust to sustain stationary flight. The XFY Pogo with its classical planar wings and SNECMA's Coleoptere with its annular wing are early examples of this type of aircraft. Many MAVs of this type have been built, like the HoverEye of Bertin Tech. (Fig. 7), the V-Bat of MLB Company (Fig. 8), the MAVion of ISAE (Fig. 9), or the Quadshot of Transition Robotics (Fig. 10). These systems are often referred to as "tail-sitters", due to their capacity to take-off and land on their tail. As indicated by the name, the main characteristics of tilt-bodies is that transition form hover to cruising flight requires the whole body to tilt (pitch down). This implies large variations of the angle of attack, which is one of the control difficulties associated with this type of system. For ducted-fan vehicles like the HoverEye and the V-bat, thrust is generated by one or two (contra-rotative) propellers located inside the duct. Torque control in hover is typically obtained via control surfaces located below these propellers, usually inside the duct so as to preserve flow interactions with the wind (see Fig. 7). Torque control in cruising flight may be aided by additional control surfaces, like for the V-Bat tail-sitter. For the MAVion, the two contra-rotative propellers and control surfaces generate thrust and torque at both hover and cruising flight. In the case of the Quadshot, the four propellers are sufficient to produce both thrust and full torque control. For more efficiency, torque control in cruising flight is also aided by control surfaces on the wing. Besides the problem of transition between hover and cruising flight, a drawback of tail-sitter systems concern payload and aerodynamic stability in hover. The wing is vertical in hover mode and therefore wind can induce important drag forces. If the CoM (Center of Mass) is not close to the aerodynamic center, important perturbation torques then appear. The worst situation with ducted fans is when such torques produce pitch-up motion (i.e., the CoM is located below the center of pressure), which makes the torque control surfaces inefficient due to the wind flow entering the duct. This is why the payload of tail-sitters is usually located above the duct. This may induce significant constraints. More details on this type of vehicles can be found in [11, 16, 18].

Tilt-rotor/Tilt-wings differ from tilt-bodies by the fact that some parts of the vehicle (wings or propellers) are no longer rigidly attached to the main body. One or several additional degree(s) of freedom allow one for the modification of the vehicle's shape with extended control possibilities. The Vertol VZ-2

Tilt-Wing of Fig. 1 is an early example of this class of vehicles with the main wing and propellers rigidly attached to each other but tilting with respect to (w.r.t.) the main body. This type of configuration can also be found at the MAV scale (like the SUAVI [4] or the QUX-02 [15] quad tilt-wings). Other types of tilt-rotors/tilt-wings MAVs have been proposed, like the tilt-rotor FW-VTOL of VTOL Tech. (Fig. 11), or the tilt-wing ConvertISIR (Fig. 12), developed in our Lab. Concerning the FW-VTOL, the four propellers can be used in hover like for a classical quadrotor, and they tilt progressively pitch down for the transition to cruising flight. With respect to tilt-bodies aircraft, the main advantage is that the wing can always keep a small angle of attack, thus making the transition easier. It should be noted that this property is not satisfied for a convertible like the Vertol VZ-2. In this case, transition still requires large variations of the angle of attack despite the additional degree of freedom. The ConvertISIR of Fig. 12 is built from a standard quadrotor, which can be seen in the center of the structure. In addition, two wings have been added to each side of the quadrotor thanks to a set of linkages. Each wing can tilt w.r.t. the propellers' plane. As in the case of the FW-VTOL, the decoupling between propellers and wings tilting angles allows for transitions with small angles of attack. Furthermore, the independent control of the two wings adds much control versatility in cruising flight.

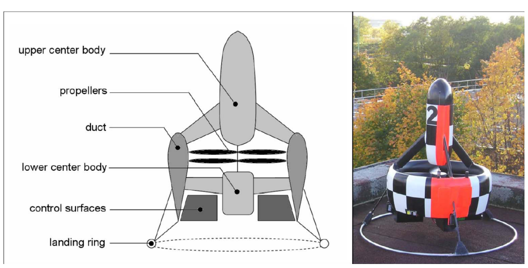

Figure 7: HoverEye Tail-sitter of Bertin Tech.

Figure 8: V-Bat Tail-Sitter of MLB Company

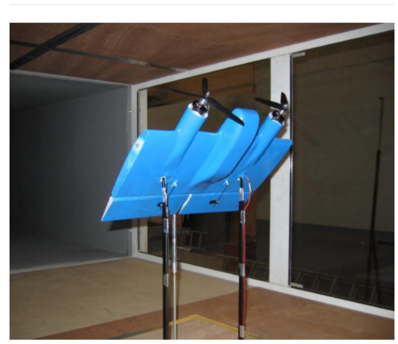

Figure 9: MAVion Tilt-body of ISAE

Figure 10: Quadshot of Transition Robotics

Figure 11: FW-VTOL Tilt-rotor of VTOL Tech.

Figure 12: ConvertISIR Tilt-wing of ISIR

3 Modeling

Most convertible MAVs share the following properties.

1. They are composed of three main components:

   $S1$: the main body;

   $S2$: the propellers, the rotation axes of which can be rigidly attached to the main body or not (tilt-rotors). From now on, it is assumed that the rotation axes of propellers all have the same direction and, in the case of tilt-rotors, that this direction in the main body frame can be parameterized by a one-dimensional parameter $s_0 \in \mathbb{S}^1$, with $\mathbb{S}^1$ the unit circle (i.e., the rotation axes move in only one direction w.r.t. the main body);

   $S3$: the moving surfaces, the primarily role of which can be torque generation (aileron, rudder, elevator of an airplane) or lift generation (e.g. wings of the ConvertISIR). It is assumed that the rotation axes of these moving surfaces is fixed in the main body frame.

2. They are underactuated in force, i.e., in body frame the control force is restricted to a linear subspace.

3. They are fully actuated in torque, i.e., in body frame the control torque is not restricted to a linear subspace.

With this in mind, the configuration space of the MAV viewed as a mechanical system is $Q = \mathbb{R}^3 \times \mathbb{SO}(3) \times \mathbb{T}^p$ with $\mathbb{R}^3 \times \mathbb{SO}(3)$ corresponding to the configuration space of the main body (3D position and orientation), and $\mathbb{T}^p$ corresponding to the configuration space of propellers and moving surfaces in the main body's frame (i.e., parametrization of propellers' rotation axes, rotation angles of propellers and moving surfaces). The notation for the configuration variables is now defined (see Fig. 13).

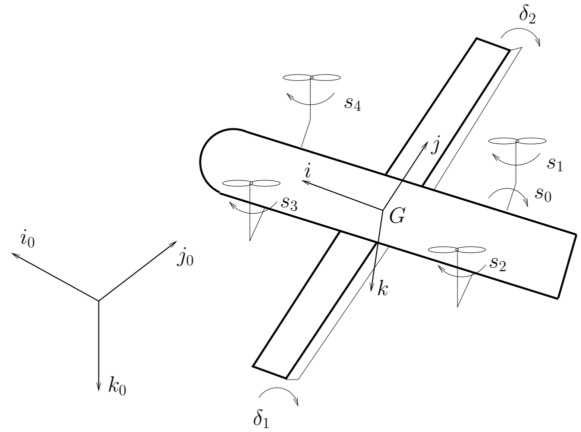

Figure 13: Schematic of notation

- $\mathcal{I} = \{O; \boldsymbol{i}_0, \boldsymbol{j}_0, \boldsymbol{k}_0\}$ denotes a fixed inertial frame with respect to (w.r.t.) which the vehicle's absolute pose is measured. This frame is chosen as the NED frame (North-East-Down) with $\boldsymbol{i}_0$ pointing to the North, $\boldsymbol{j}_0$ pointing to the East, and $\boldsymbol{k}_0$ pointing to the center of the Earth.

- $\mathcal{B} = \{G; \boldsymbol{i}, \boldsymbol{j}, \boldsymbol{k}\}$ denotes a frame attached to the main body, with G the vehicle's center of mass. It is assumed here that G is a fixed point in the body frame. This may not always be true, especially for tilt-rotors/tilt-wings MAVs since their shape can change, but this is a reasonable assumption in first approximation.

- The vector of coordinates of G w.r.t. $\mathcal{I}$ is denoted as p. The rotation matrix from $\mathcal{B}$ to $\mathcal{I}$ is denoted as R.

- Beside the parameter s_0 used to parameterize the direction of the propellers' axes in body frame, $s_1, \ldots s_{n_p}$ denote the rotation angles of the propellers, with n_p the number of propellers, and $\delta_1, \ldots \delta_{n_s}$ denote the rotation angles of the moving surfaces, with n_s the number of these surfaces.

The configuration vector is thus given by $q = (p, R, s_0, s_1, \cdots, s_{n_p}, \delta_1, \cdots, \delta_{n_s})$. The variables s_i, δ_j correspond to the "shape variables" of the MAV. From these definitions one can readily define the MAV's velocity vector expressed in inertial frame: $v = \dot{p}$, and its angular velocity vector expressed in body frame: ω such that $\dot{R} = RS(\omega)$ with $S(.)$ the skew-symmetric matrix associated with the cross product, i.e., $S(\omega)y = \omega \times y$ for all y.

3.1 Dynamic modeling

The dynamical equations are derived from Newton-Euler equations:

$$\begin{aligned} m\dot{v} &= mge_3 + F \\ J\dot{\omega} &= -S(\omega)J\omega + \Gamma \end{aligned} \tag{1}$$

with m the vehicle's mass, here assumed to be constant, g the gravitational constant, $e_3 = (0, 0, 1)^T$, F the resultant of all aerodynamic forces acting on the vehicle, expressed in inertial frame, J the inertia matrix, and Γ the vector of coordinates of the torques applied to the main body, expressed in body frame. The above dynamical model is incomplete since the dynamics of the variables s_i, δ_j is not specified. Usually, each of these configuration variables is actuated (servos for propellers' rotation axis direction, brushless motors for propellers, servos for moving surfaces). Furthermore, for MAVs the actuation dynamics is often very fast w.r.t. the MAV's main body dynamics. We will make this assumption from now on and assume that the following values can be considered as control input: propellers' rotation axis direction angle s_0, propellers' rotational velocities $\varpi_1 := \dot{s}_1, \cdots, \varpi_n := \dot{s}_{n_p}$, moving surfaces orientation angle $\delta_1, \cdots, \delta_{n_s}$.

The modeling of aerodynamic forces and torques acting on a body immersed in a fluid is the basic ingredient for specifying the aerodynamic force F and the torque Γ. This is a huge and complex topic that has been addressed with a variety of techniques: Computational Fluid Dynamics (CFD), Wind-Tunnel (WT) measurements, Analytical methods. We recall hereafter some basic elements of aerodynamic modeling. Consider a body moving at velocity v and denote by v^a the air velocity, i.e. $v^a = v - v^w$ with v^w the wind's velocity. The aerodynamic force F_a exerted on the body is typically decomposed as $F_a = F_L + F_D$ where the *lift force* F_L is the component perpendicular to v^a and the *drag force* F_D is the component parallel to v^a. These two components can be written as follows:

$$F_L = \frac{1}{2}\rho\Sigma\, C_L|v_a|(v^a)^\perp, \quad F_D = -\frac{1}{2}\rho\Sigma\, C_D|v^a|v^a \tag{2}$$

with ρ the air density, Σ an area associated with the body, and $(v^a)^\perp$ a vector orthogonal to v^a with amplitude $|v^a|$. C_D and C_L are the *aerodynamic characteristics* of the body, i.e. the so-called *drag* and *lift* coefficients. The main difficulty consists in specifying these coefficients and the direction of $(v^a)^\perp$:

- Aerodynamic characteristics depend on several variables: Reynolds number, Mach number, and orientation of the air velocity vector w.r.t. the body. From a mathematical viewpoint the latter is an element of the unit sphere and it is usually specified by the so-called angle of attack α and side slip angle β. A major difficulty is to specify the dependence of C_L and C_D on α and β. This is already a challenging task under steady flight conditions (i.e., constant α and β) and one usually has to resort to CFD or WT methods. A deeper difficulty comes from the fact that C_L and C_D are not just functions of the variables α and β but functionals of $\alpha(.)$ and $\beta(.)$: a variation of α or β at time τ modifies the pressure distribution around the body in all subsequent times $t \geq \tau$, in a domain defined by the sound's speed. Thus, for subsonic flight, the aerodynamic forces acting on the body at time t depend on past time values $\tau \leq t$, i.e. C_L and C_D at time t depend not only on $\alpha(t)$ and $\beta(t)$ but also on $\alpha(\tau)$ and $\beta(\tau)$ for $\tau \leq t$. Such a complexity cannot be handled easily analytically and the classical approach (see [5, Ch. 5] and the references therein) consists in approximating the functional dependence by a dependence on the successive derivatives at time t, i.e. C_L and C_D at time t are expressed in term of $\alpha(t), \beta(t), \dot{\alpha}(t), \dot{\beta}(t), \ddot{\alpha}(t), \ddot{\beta}(t), \cdots$. For flight dynamics model, dependence on second and higher-order derivatives is usually omitted so that C_L and C_D become functions of $\alpha, \beta, \dot{\alpha}, \dot{\beta}$ where dependence on $\dot{\alpha}, \dot{\beta}$ is associated with unsteady aerodynamic effects. One may question the importance of taking into account such unsteady effects. This depends essentially on the dynamics of the system. Due to their small size, however, the rotational dynamics of MAVs can be very fast, thus leading to large values of $\dot{\alpha}, \dot{\beta}$. For example, a WT study conducted in [2] on a F-18 aircraft model showed overshoot of the lift coefficient of up to 40% w.r.t. static values due to pitching rate. This value is large enough to deserve attention. Another difficulty concerns the dependence of the aerodynamic characteristics on the Reynolds number. MAVs evolve in a range of relatively low Reynolds numbers (typically less than 200 000), and many different flow behaviors can be found in this range with strong impact on the aerodynamic characteristics (see [14] for more details).

- The direction of the lift force, defined by $(v^a)^\perp$, is difficult to specify in general. Most of the time, MAVs possess symmetry planes which allow one to deduce information on $(v^a)^\perp$, especially when $\beta = 0$. For significant values of the side slip angle, however, one also has to resort to CFD or WT methods to get more information of the lift force direction.

We will not go further into these aerodynamic issues (this is out of the scope of this paper and expertise of the author) but they cannot be disregarded if aggressive flight capacities are required.

Going back to System (1), a model of F that ignores unsteady aerodynamic effects and dependence on Reynolds number and Mach number can be specified:

$$F = F_0(R, v^a) - \sum_{i=1}^{n_p} b_i \varpi_i^2 R Q(s_0) e_3 + \sum_{j=1}^{n_s} F_j(R, \delta_j, v_j^a)$$

F_0 corresponds to the aerodynamic force acting on the main body (expressed in inertial frame), with the dependence on the angle of attack/side slip angle and air-velocity written as a dependence on R and v^a (this is an over-parameterization that simplifies the notation). The terms in the first sum correspond to the lift forces exerted on the propellers, with $b_i > 0$ $(i = 1, \cdots, n_p)$ associated with the lift coefficient of propeller i, and $Q(s_0)e_3$ corresponding to the direction of these lift forces in body frame. $Q(s_0)$ is a rotation matrix parameterized by the rotation angle s_0, with $Q(s_0^*)$ the identity matrix if s_0^* corresponds to the propellers configuration at hover (i.e., vertical lift force). It should be remarked at this point that the effects of v^a on the propellers aerodynamics is here neglected, i.e. it is assumed that the air-velocity on the propellers' blades is only induced by the propellers' rotational velocities ϖ_i (which is the case only in hover and without wind). This effect can be significant [6], all the more when the speed controller of propellers' brushless motors is not accurate enough. A finer modeling that incorporates such effects can be found in [13]. Finally, F_j $(j = 1, \cdots, n_s)$ corresponds to the aerodynamic force acting on the moving surface j. Note that v_j^a, the air-velocity on moving surface j, is not necessarily equal to v^a. This distinction is important to take aerodynamic interactions into account.
Similarly, a first model of Γ can be specified as:

$$\begin{aligned}\Gamma \;=\;& \Gamma_0(R, v^a) \\ & - \sum_{i=1}^{n_p} b_i \varpi_i^2 \ell_i \times Q(s_0) e_3 - \sum_{i=1}^{n_p} \kappa_i \varpi_i^2 Q(s_0) e_3 \\ & + \sum_{j=1}^{n_s} \Gamma_j(R, \delta_j, v_j^a)\end{aligned}$$

Γ_0 is associated with the moment of aerodynamic forces acting on the main body (expressed in body frame). The terms in the first sum correspond to the torque induced on the main body by lift forces acting on the propellers, with ℓ_i denoting the coordinates of the center of the i-th propeller in the body frame. The terms in the second sum correspond to the torque induced on the main body by drag forces acting on the propellers (moment around the propellers' axis), with κ_i $(i = 1, \cdots, n_p)$ a parameter associated with the drag coefficient of propellers i, the sign of which depends on the direction of rotation of propeller i (i.e. clockwise or anti-clockwise). Finally, Γ_j $(j = 1, \cdots, n_s)$ corresponds to the torque induced on the main body by aerodynamic forces acting on the control surface j (including aerodynamic lift, drag, and moment). Again, effects of v^a on the propellers aerodynamics is here neglected. We have also implicitly assumed that so-called *gyroscopic torques* are negligible.
To further specify the expression of F and Γ would require to further specify $F_0, F_j, \Gamma_0, \Gamma_j$ by introducing expressions of aerodynamic lift, drag, and moment. In order to avoid making this paper too technical, we will not delve into this level of details.

4 Feedback control

The control problem considered in this section is the stabilization of the MAV's position vector p to a reference trajectory p_r. There is currently no general method that can address this problem for the class of systems here considered, even with the modeling assumptions of the previous section. Therefore, the objective of this section is not to provide a control solution for this system (this remains to be achieved), but to provide a general overview of the main cases of interest, possible control solutions, and difficulties.

4.1 Multirotors

Multirotors (quadrirotors, hexarotors, etc) are usually not classified among convertible UAVs but they satisfy the modeling assumptions of the previous section (they are composed of a main body and propellers). Furthermore, their control provides significant insight. We briefly review this case (see, e.g., [12] for more details). We consider here[1] multirotors with rotation axes of propellers fixed in body frame and parallel to k. In other words, the configuration variables are limited to (p, R) and the only control variables are the propellers rotational velocities. The vectors F and Γ then reduce to

$$\begin{aligned} F &= F_0(R, v^a) - \sum_{i=1}^{n_p} b_i \varpi_i^2 R e_3 \\ \Gamma &= \Gamma_0(R, v^a) - \sum_{i=1}^{n_p} b_i \varpi_i^2 \ell_i \times e_3 - \sum_{i=1}^{n_p} \kappa_i \varpi_i^2 e_3 \end{aligned}$$

When the number of propellers n_p is at least equal to four, under a physically reasonable location of the propellers on the MAV and choice of rotational direction

[1] The control principle of multirotors with tiltable propellers does not differ significantly from the case here considered (see [7] for details).

of the propellers (i.e., depending on the value of the vectors ℓ_i and the parameters κ_i), the linear mapping

$$\begin{pmatrix} \varpi_1^2 \\ \vdots \\ \varpi_{n_p}^2 \end{pmatrix} \longmapsto \begin{pmatrix} \sum_{i=1}^{n_p} b_i \varpi_i^2 \\ \sum_{i=1}^{n_p} b_i \varpi_i^2 \ell_i \times e_3 + \sum_{i=1}^{n_p} \kappa_i \varpi_i^2 e_3 \end{pmatrix}$$

is onto a neighborhood of any vector of the form $(c, 0, 0, 0)^T$ with $c > 0$. This allows one to perform a change of control variables and rewrite F and Γ as follows:

$$\begin{array}{rcl} F & = & F_0(R, v^a) - T_c R e_3 \\ \Gamma & = & \Gamma_0(R, v^a) + \Gamma_c \end{array} \tag{3}$$

with

$$T_c := \sum_{i=1}^{n_p} b_i \varpi_i^2 \tag{4}$$

the thrust control and Γ_c a torque control variable. The dynamical system (1) then reduces to

$$\begin{array}{rcl} m\dot{v} & = & mge_3 + F_0(R, v^a) - T_c R e_3 \\ J\dot{\omega} & = & -S(\omega) J\omega + \Gamma_0(R, v^a) + \Gamma_c \end{array} \tag{5}$$

with T_c and Γ_c as control variables. For multirotors, it is usually assumed that F_0 little depends on R. This is justified by the absence of wings that could induce significant lift forces. Under this assumption, the translation dynamics simplifies as

$$m\dot{v} = mge_3 + F_0(v^a) - T_c R e_3$$

with F_0 accounting for drag forces (typically, $F_0(v_a) = -c_0 v^a |v^a|$ with $c_0 > 0$). The control design then proceeds essentially as follows (see [17, 8, 9] for details). Let $\tilde{p} := p - p_r$ denote the tracking error. Then, from the above equation,

$$m\ddot{\tilde{p}} = mge_3 + F_0(v^a) - m\ddot{p}_r - T_c R e_3 \tag{6}$$

Assume for a moment that

$$T_c R e_3 = mge_3 + F_0(v^a) - m\ddot{p}_r - \beta(\tilde{p}, \dot{\tilde{p}}) \tag{7}$$

Then, (6) becomes $m\ddot{\tilde{p}} = -\beta(\tilde{p}, \dot{\tilde{p}})$. Choosing $\beta(\tilde{p}, \dot{\tilde{p}})$ such that the origin of this system is asymptotically stable (e.g., a simple second-order linear controller) then ensures that $\tilde{p}$ exponentially converges to zero. Now, (7) cannot be instantaneously satisfied but it readily defines the "thrust control"

$$T_c = \| mge_3 + F_0(v^a) - m\ddot{p}_r - \beta(\tilde{p}, \dot{\tilde{p}}) \|$$

and a desired thrust direction

$$(Re_3)_d := \frac{mge_3 + F_0(v^a) - m\ddot{p}_r - \beta(\tilde{p}, \dot{\tilde{p}})}{\| mge_3 + F_0(v^a) - m\ddot{p}_r - \beta(\tilde{p}, \dot{\tilde{p}}) \|} \tag{8}$$

There remains to stabilize the thrust direction Re_3 to $(Re_3)_d$ via the control Γ_c, which is not difficult from a theoretical point of view since Eq. 5 shows that the rotational dynamics is fully actuated. Eq. (8) suggests a difficulty if the denominator of the right-hand side vanishes since in this case the desired thrust direction is no longer well defined. This is not an issue in normal flight conditions because the dominant term of this denominator is mge_3. In extreme flight conditions, however, nothing forbids that this denominator vanishes.

4.2 Tilt-bodies

Since the propellers are fixed in the body frame, the general expressions of F and Γ given in Section 3 simplify as:

$$\begin{array}{rcl} F & = & F_0(R, v^a) - \sum_{i=1}^{n_p} b_i \varpi_i^2 R e_3 + \sum_{j=1}^{n_s} F_j(R, \delta_j, v_j^a) \\ \Gamma & = & \Gamma_0(R, v^a) - \sum_{i=1}^{n_p} b_i \varpi_i^2 \ell_i \times e_3 - \sum_{i=1}^{n_p} \kappa_i \varpi_i^2 e_3 \\ & & + \sum_{j=1}^{n_s} \Gamma_j(R, \delta_j, v_j^a) \end{array}$$

This form is more general than the multirotor case and therefore, it allows for many different configurations. The thrust is generated by one, two (HoverEye, MAVion), or more (Quadshot) propellers. Control torques are generated by propellers and control surfaces, located below the propellers, that generate complementary torques thanks to the incoming propellers' flow. An important point is that these control surfaces have little effect on the linear dynamics because of their limited size. Under normal flight conditions (essentially if the total thrust does not vanish and the control surfaces' angles of attack remain small), the nonlinear mapping

$$\begin{pmatrix} \varpi_1^2 \\ \vdots \\ \varpi_{n_p}^2 \\ s_1 \\ \vdots \\ s_{n_s} \end{pmatrix} \longmapsto \begin{pmatrix} \sum_{i=1}^{n_p} b_i \varpi_i^2 R e_3 \\ \sum_{i=1}^{n_p} b_i \varpi_i^2 \ell_i \times e_3 + \sum_{i=1}^{n_p} \kappa_i \varpi_i^2 e_3 \cdots \\ \cdots - \sum_{j=1}^{n_s} \Gamma_j(R, \delta_j, v_j^a) \end{pmatrix}$$

is onto a neighborhood of any vector of the form $(c, 0, 0, 0)^T$ with $c > 0$. This allows one to rewrite

F and Γ as follows:

$$\begin{aligned} F &= F_0(R, v^a) - T_c R e_3 + \sum_{j=1}^{n_s} F_j(R, \delta_j, v_j^a) \\ \Gamma &= \Gamma_0(R, v^a) + \Gamma_c \end{aligned} \quad (9)$$

with T_c still defined by (4). Note that some of (if not all) the variables δ_j can be constrained, through the change of coordinates, by the values of T_c and Γ_c. In this case, they are no longer available control variables. Eq. (9) is very similar to (3). The term $\sum_{j=1}^{n_s} F_j(R, \delta_j, v_j^a)$, referred to as "small body forces", can often be neglected in first approximation due to the size of the control surfaces (as mentioned above). Then, the dynamical model reduces to (5). The major difference w.r.t. the case of multirotors is that one can no longer assume that F_0 does not depend on R, since tilt-body MAVs are endowed with wings. The main consequence concerns the control methodology used for multirotors. When trying to apply it to the present case, a difficulty occurs because Eq. (8) becomes

$$(Re_3)_d := \frac{mge_3 + F_0(R_d, v^a) - m\ddot{p}_r - \beta(\tilde{p}, \dot{\tilde{p}})}{\| mge_3 + F_0(R_d, v^a) - m\ddot{p}_r - \beta(\tilde{p}, \dot{\tilde{p}}) \|} \quad (10)$$

Since both terms of this equality depend on R_d, existence and uniqueness of the desired "thrust direction" is no longer granted. In particular, when $\beta \equiv 0$, the underlying problem is the feasibility of the trajectory p_r. While any trajectory p_r is feasible for a quadrotor (notwithstanding control limitations), it becomes much more difficult to assert the feasibility of such a trajectory for a tilt-body MAV. This is a major issue that deserves complementary remarks.

1. The problem of existence and uniqueness of the desired thrust direction does not concern low velocity flight because aerodynamic forces vanish with v^a. As a consequence, the term $F_0(R_d, v^a)$ remains small as long as v^a is small and one easily verifies that the desired thrust direction is well defined in this case. This may explain why several successful flight tests of tilt-body MAVs at low/moderate speeds have been reported. Transition to high-speed flight is another issue.

2. A deeper study of this problem can be found in [20], where it is shown that stall effect (in particular) induces multiple solutions to Eq. (10) on some velocity range, with discontinuities of these solutions for some smooth variations of v^a.

3. It has recently been shown in [21] that for a class of axi-symmetric bodies that satisfy some conditions on lift and drag aerodynamic characteristics, the solution to Eq. (10) is well defined and unique. This allows for the extension of the multirotors control methodology to this class of systems.

4. The above remarks show the intrinsic difficulty of addressing the stabilization problem of tilt-bodies generically (i.e., in the sense of making no assumption on the reference trajectory p_r). Then, as far as transition from hover to cruising flight is concerned, one may wonder whether this can be achieved via specific trajectories p_r. Indeed, a strategy used from the very beginning of tilt-body aircraft consists in transitioning along trajectories that involve large vertical variations, so as to keep the angle of attack small. Horizontal transitions have also been demonstrated on some tilt-bodies (see, e.g. [10]), based on the local stabilization of an equilibrium trajectory determined experimentally in wind-tunnel after trials and errors. This type of approach remains experimentally expensive, however, with no guarantee of success a priori since the existence of such equilibrium trajectories is not granted.

4.3 Tilt-rotors/tilt-wings

This is the more general case, which allows for a huge variety of possibilities. By proceeding as in the previous cases, it is normally possible to simplify the expression of F and Γ by a change of control variables as follows (compare with (3)):

$$\begin{aligned} F &= F_0(R, v^a) - T_c R Q(s_0) e_3 + \sum_{j=1}^{n_s} F_j(R, \delta_j, v_j^a) \\ \Gamma &= \Gamma_0(R, v^a) + \Gamma_c \end{aligned}$$

with T_c defined as above and Γ_c the new torque control variable. As in the case of tilt-body vehicles, some of the variables δ_j might be constrained, through the change of control variable, by the values of T_c and Γ_c. Some particular configurations have been more specifically investigated.

Tilt-rotors: A first configuration is when the moving surfaces are only used for torque generation. An example is given by the FW-VTOL of Fig. 11. Then, as in the case of tilt-bodies, the term $\sum_{j=1}^{n_s} F_j(R, \delta_j, v_j^a)$ can essentially be neglected and the expression of F reduces to

$$F = F_0(R, v^a) - T_c R Q(s_0) e_3$$

This expression is similar to the first equality in (3) with the additional control parameter s_0. The important point is that the resulting force can be partially modified via s_0 without modifying the main body's orientation (matrix R). This is the main advantage of tilt-body vehicles, which allows for transitions from hover to cruising flight while keeping a constant pitch angle of the main body. This much alleviates the problem mentioned above for tilt-bodies and suggests another control strategy, where the main body's pitch angle is kept at a constant value thanks to the control variable s_0 so as to best benefit from lift (small angle of attack), and the trajectory tracking is achieved via the control provided by the propellers. Since s_0 is uni-dimensional the problem persists for the roll control but it is much less drastic because the amplitude of lateral forces is typically less important. Furthermore a sound control strategy consists in reducing as much as possible the side slip angle, via the yaw control torque, in order to keep these forces small.

Tilt-wings: Another configuration is when the rotors are rigidly attached to the main body but the wings can be tilted independently. An example is given by the ConvertISIR of Fig. 12. The dependence of F_0 on the rotation matrix can usually be neglected in first approximation since the wings account for the major part of aerodynamic forces. The expression of F reduces to

$$F = F_0(v^a) - T_c R e_3 + \sum_{j=1}^{n_s} F_j(R, \delta_j, v_j^a)$$

This case is very similar to the tilt-rotors case because it also allows for transitions from hover to cruising flight while keeping wings' angles of attack small. The idea is to compensate the pitching of the main body so as to maintain the wing at a desired angle of attack. The variables δ_j are used to this purpose, i.e., δ_j is defined as a function of R to decouple the wing pitch angle from the main body's pitch angles. The control approach used for multirotors can again be used since the control δ_j eliminates the dependence of F_j on R. Like in the case of tilt-rotors, this much alleviates the problem of ill-definition of the thrust direction. Like in the case of tilt-rotors, also, this dependence is not completely eliminated due to the roll degree of freedom. Again, the yaw control torque can be used to keep these lateral forces small. More details on the control of the ConvertISIR can be found in [19].

Tilt-rotors/wings: The final case is when the rotors are rigidly attached to the wings and the set rotors/wings can be tilted w.r.t. the main body. An example is given by the Vertol VZ2 of Fig. 1. Since the rotors and wings are rigidly attached, there exist functions $\bar{F}_j$ such that F can be rewritten as follows:

$$F = F_0(v^a) - T_c R Q(s_0) e_3 + \sum_{j=1}^{n_s} \bar{F}_j(RQ(s_0), v_j^a)$$

Note that we again assume here that F_0 does not depend on R. Despite the additional degree of freedom s_0, the problem of ill-definition of the thrust direction here remains because changing the thrust force direction through $RQ(s_0)$, either by a change of R or by a change of s_0, modifies at the same time the aerodynamic forces on the wings. Thus, from a control point of view this type of configuration remains close to the tilt-body configuration, with the associated control difficulties.

5 Conclusion and open problems

We have provided an overview of MAV convertible structures and associated modeling and control issues. We believe that this is a very rich field of investigation for the control/robotics community. Major issues concern a better understanding of the aerodynamics of these systems, the design of control models that can account for this aerodynamic in a large range of flight conditions (large angles of attack, fast rotational dynamics), and the design of feedback control laws that fully exploit such models. For example, unsteady aerodynamic effects have not been considered when dealing with control aspects. The interested reader will easily identify the additional difficulties that they can generate for the control design (for example, by allowing the functions F_0, F_j to depend not only on R but also on its derivative, i.e., on the angular velocity vector ω). Another problem, closer to the robotics community interests, concerns a good allocation of control resources, since most convertible UAVs have redundant actuation for some degrees of freedom. For example, the pitch and yaw angles of the Quadshot can be modified either by controlling the propellers' thrust, or by controlling the control surfaces. Finally, another large field of investigation concerns state estimation, which has been totally concealed here. In particular, estimation of wind and its aerodynamic effects is an important issue at this scale.

References

[1] J.M. Basset, A. Tremolet, and T. Lefebvre. Rotary wings uavs presizing: Past and present methodological approaches at onera. *Onera Aerospace Lab*, 8, 2014.

[2] J.M. Brandon. Dynamic stall effects and applications to high performance aircraft. Technical Report R-776, AGARD, 1991.

[3] S.L. Brunton. *Unsteady aerodynamic models for agile flight at low reynolds numbers*. PhD thesis, Princeton University, 2012.

[4] E. Cetinsoy, S. Dikyar, C. Hancer, K.T. Oner, E. Sirimoglu, M. Unel, and M.F. Aksit. Design and construction of a novel quad tilt-wing uav. *Mechatronics*, 22:723–745, 2012.

[5] B. Etkin and L.D. Reid. *Dynamics of flight-Stability and Control*. Wiley, third edition, 1997.

[6] G.M. Hoffmann, H. Huang, S.L. Waslander, and C.J. Tomlin. Quadrotor helicopter flight dynamics and control: Theory and experiment. In *Proc. of the AIAA Guidance, Navigation, and Control Conference*, volume 2, 2007.

[7] M.-D. Hua, T. Hamel, P. Morin, and C. Samson. Control of vtol vehicles with thrust-tilting augmentation. *Automatica*, 52:1–7, 2015.

[8] M.D. Hua, T. Hamel, P. Morin, and C. Samson. A control approach for thrust-propelled underactuated vehicles and its application to vtol drones. *IEEE Trans. on Automatic Control*, 54:1837–1853, 2009.

[9] M.D. Hua, T. Hamel, P. Morin, and C. Samson. Introduction to feedback control underactuated vtol vehicles. *IEEE Control Systems Magazine*, pages 61–75, 2013.

[10] M. Itasse, J.M. Moschetta, Y. Ameho Yann, and R. Carr. Equilibrium transition study for a hybrid mav. *International Journal of Micro Air Vehicles*, 3:229–246, 2011.

[11] E.N. Johnson and M.A. Turbe. Modeling, control, and flight testing of a small-ducted fan aircraft. *Journal of guidance, control, and dynamics*, 29(4):769–779, 2006.

[12] R. Mahony, V. Kumar, and P. Corke. Multirotor aerial vehicles: Modeling, estimation, and control of quadrotor. *IEEE Robotics and Automation Magazine*, 19:20–32, 2012.

[13] P. Martin and E. Salaün. The true role of accelerometers feedback in quadrotor control. In *IEEE Conf. on Robotics and Automation (ICRA)*, pages 1623–1629, 2010.

[14] T.J. Mueller. Aerodynamics measurements at low reynolds numbers for fixed-wing micro-air vehicle. Technical report, RTO AVT/KTI special course on development and operation of UAVs for civil and military applications, 1999.

[15] K. Muraoka, N. Okada, and D. Kubo. Quad tilt wing vtol uav: aerodynamic characteristics and prototype flight test. In *AIAA Infotech@ Aerospace Conference*, 2009.

[16] J.-M. Pflimlin, P. Binetti, P. Souères, T. Hamel, and D. Trouchet. Modeling and attitude control analysis of a ducted-fan micro aerial vehicle. *Control Engineering Practice*, 18:209–218, 2010.

[17] J.-M. Pflimlin, T. Hamel, P. Souères, and R. Mahony. A hierarchical control strategy for the autonomous navigation of a ducted fan flying robot. In *IEEE Conf. on Robotics and Automation (ICRA)*, pages 2491– 2496, 2006.

[18] J.-M. Pflimlin, P. Souères, and T. Hamel. Position control of a ducted fan vtol uav in crosswind. *International Journal of Control*, 80(5):666–683, 2007.

[19] D.-K. Phung. *Conception, modeling, and control of a convertible mini-drone*. PhD thesis, Université Pierre et Marie Curie, 2015.

[20] D. Pucci. Flight dynamics and control in relation to stall. In *American Control Conference*, pages 118–124, 2012.

[21] D. Pucci, T. Hamel, P. Morin, and C. Samson. Nonlinear feedback control of axisymmetric aerial vehicles. *Automatica*, 53:72–78, 2015.